

Published in final edited form as:

Toxicol Appl Pharmacol. 2009 November 1; 240(3): 348–354. doi:10.1016/j.taap.2009.07.021.

Troglitazone, but not rosiglitazone, damages mitochondrial DNA and induces mitochondrial dysfunction and cell death in human hepatocytes

Lyudmila I. Rachek^{1,*}, Larysa V. Yuzefovych¹, Susan P. LeDoux¹, Neil L. Julie², and Glenn L. Wilson¹

¹Department of Cell Biology and Neuroscience, College of Medicine, University of South Alabama, Mobile, Alabama 36688

²Shady Grove Adventist Hospital, Rockville, MD 20850

Abstract

Thiazolidinediones (TZDs), such as troglitazone (TRO) and rosiglitazone (ROSI), improve insulin resistance by acting as ligands for the nuclear receptor peroxisome proliferator-activated receptor- γ (PPAR γ). TRO was withdrawn from the market because of reports of serious hepatotoxicity. A growing body of evidence suggests that TRO caused mitochondrial dysfunction and induction of apoptosis in human hepatocytes but its mechanisms of action remain unclear. We hypothesized that damage to mitochondrial DNA (mtDNA) is an initiating event involved in TRO-induced mitochondrial dysfunction and hepatotoxicity. Primary human hepatocytes were exposed to TRO and ROSI. The results obtained revealed that TRO, but not ROSI at equimolar concentrations, caused a substantial increase in mtDNA damage and decreased ATP production and cellular viability. The reactive oxygen species (ROS) scavenger, N-acetyl cystein (NAC), significantly diminished the TRO-induced cytotoxicity, suggesting involvement of ROS in TRO-induced hepatocyte cytotoxicity. The PPAR γ antagonist (GW9662) did not block the TRO-induced decrease in cell viability, indicating that the TRO-induced hepatotoxicity is PPAR γ -independent. Furthermore, TRO induced hepatocyte apoptosis, caspase-3 cleavage and cytochrome c release. Targeting of a DNA repair protein to mitochondria by protein transduction using a fusion protein containing the DNA repair enzyme Endonuclease III (EndoIII) from *Escherichia coli*, a mitochondrial translocation sequence (MTS) and the protein transduction domain (PTD) from HIV-1 TAT protein protected hepatocytes against TRO-induced toxicity. Overall, our results indicate that significant mtDNA damage caused by TRO is a prime initiator of the hepatotoxicity caused by this drug.

Keywords

Troglitazone; rosiglitazone; apoptosis; mitochondrial DNA; mitochondria; human hepatocytes

© 2009 Elsevier Inc. All rights reserved.

*To whom correspondence should be addressed: Department of Cell Biology and Neuroscience, University of South Alabama, Mobile, AL 36688, USA. Tel # (251) 460-6960; Fax # (251) 414-8241; lrachek@jaguar1.usouthal.edu.

Publisher's Disclaimer: This is a PDF file of an unedited manuscript that has been accepted for publication. As a service to our customers we are providing this early version of the manuscript. The manuscript will undergo copyediting, typesetting, and review of the resulting proof before it is published in its final citable form. Please note that during the production process errors may be discovered which could affect the content, and all legal disclaimers that apply to the journal pertain.

Introduction

The antidiabetic thiazolidinediones (TZDs) troglitazone (TRO) and rosiglitazone (ROSI) have been found to improve insulin resistance, leading to reduced blood glucose and insulin levels and the preservation of pancreatic function (1-3). It is believed that TZDs work by sensitizing the action of insulin by acting as ligands for the nuclear peroxisome proliferator-activated receptor- γ (PPAR γ) (4-5). TRO was the first member of the TZDs developed to treat type 2 diabetes. However, it was withdrawn from the market in 2000 because of reports of serious hepatotoxicity. Another PPAR γ agonist, ROSI, is still on the market. The rapid onset of changes induced by TRO indicates that it has effects that are not mediated by PPAR γ . Although a number of hypotheses have been proposed to explain TRO-induced cell injury, including the formation and accumulation of toxic metabolites, mitochondrial dysfunction and oxidant stress, inhibition of the bile salt transporter and bile acid toxicity, and the induction of apoptosis (rev. in 6), an initiating mechanism has yet to be fully identified.

Previous studies performed by other groups indicated that TRO induced mitochondrial dysfunction during the development of toxicity (7-11). As a result of TRO-induced mitochondrial dysfunction, it has been reported that the production of reactive oxygen species (ROS) is increased in human hepatocytes (10,12). Also, there is a concomitant rise in the TRO-induced initiation of apoptosis in different cell types (13,14). However, the mechanisms linking TRO-induced oxidative stress to hepatic cell injury and the cellular targets for TRO have not been fully identified. We hypothesized that one of these targets might be mitochondrial DNA (mtDNA). We proposed that damage to mtDNA is an initiating event involved in TRO-induced mitochondrial dysfunction and hepatotoxicity. To test this hypothesis, primary human hepatocytes were exposed to TRO and ROSI. The results obtained revealed that TRO, but not ROSI, when used at similar concentrations, caused a significant increase in mtDNA damage which caused a subsequent decrease in ATP levels and ultimately led to a loss of cellular viability. Furthermore, TRO induced apoptosis via a mitochondrial pathway in primary cultures of human hepatocytes. In addition, we found that targeting the DNA repair protein Endonuclease III (EndoIII) to mitochondria ameliorates TRO-induced toxicity, thus demonstrating the involvement of mtDNA damage in TRO-induced toxicity.

Materials and methods

Reagents

Human hepatocyte complete media (HHCM) was obtained from Celprogen (San Pedro, CA). TRO (purity>98%) was obtained from Sigma (St. Louis, MO) or Cayman Chemical (Ann Arbor, MI); ROSI and GW9662 were from Cayman Chemical (Ann Arbor, MI). The CellTiter 96 assay kit was obtained from Promega (Madison, WI), The Cell Death Detection ELISA^{PLUS} kit was from Roche Diagnostics Corporation (Indianapolis, IN). The ATP bioluminescence assay kit was from Roche Molecular Biochemicals (Mannheim, Germany). T25 and T75 tissue culture flasks, 60 or 100 mm diameter dishes, 24-well plates coated with hepatocyte growth matrix were obtained from Celprogen (San Pedro, CA), polyornithine and NAC were from Sigma (St.Louis, MO). Apurinic site-containing oligonucleotide for Endonuclease III activity assay was from Trevigen (Gaithersburg, MD).

Cell culture and drug treatment

Primary cultures of human hepatocytes were obtained from Celprogen (San Pedro, CA). Cells were grown in HHCM in an atmosphere of 5% CO₂ at 37°C. Human hepatocytes were grown in T25 or T75 flasks. For experiments, human hepatocytes were plated in 60 or 100 mm diameter dishes or 24-well plates coated with hepatocyte growth matrix or previously coated with polyornithine (1 μ g/ml). Cells were grown until 80-100% confluency and cultures were

used for experiments ~2 days after plating. Human hepatocytes were exposed to different concentrations (5-50 μM) of TRO or ROSI in HHCM for 24 h in a 5% CO_2 atmosphere at 37° C. Stock solutions of TRO, ROSI and GW9662 were prepared in dimethylsulfoxide (DMSO). Control cultures not treated with TRO, ROSI or GW9662 received the same concentration of DMSO as in the compound treated cultures. Cultures containing either GW9662 (10 μM) or NAC (10mM) were pretreated for 15 min prior to TRO addition.

Assay for mtDNA damage

Human hepatocytes were exposed to either TRO or ROSI as described above. After treatment cells were lysed in 10 mM TRIS-HCl (pH 8.0), 1 mM EDTA (pH 8.0), 0.5% SDS and 0.3 mg/ml proteinase K overnight at 37°C. DNA isolation and quantitative alkaline Southern blots were performed as previously described (16,17) with some modifications. High molecular weight DNA was extracted with phenol, treated with RNase (to a final concentration of 1 $\mu\text{g}/\text{ml}$), and digested to completion with *Bam*HI (10 units/ μg of DNA overnight). Digested samples were precipitated, resuspended in TE buffer, and precisely quantified using a Hoefer TKO 100 minifluorometer and TKO standard kit. Samples containing 5 μg DNA were heated at 70° C for 15 min and then cooled at room temperature for 20 min. A sodium hydroxide solution then was added to a final concentration of 0.1 N and samples were incubated for 15 min at 37°C. This alkali treatment produced single strand breaks at all abasic or sugar-modified sites in the DNA. Gel electrophoresis and vacuum transfer were carried out as described previously (16, 17). Following prehybridization, membranes were hybridized with a denatured PCR-generated mitochondrial probe (16,17), washed according to the manufacturer's suggestions, and autoradiographed. Autoradiograms were scanned for hybridization band intensity. MtDNA damage was assessed as the diminished intensity in the 16.5 kb restriction band, as compared to control bands (DNA isolated from cultures not treated with TRO or ROSI). A decrease in band intensity indicated that DNA breaks had caused smaller size fragments which migrated further down in the gel and thus reduced the number of full size restriction fragments. The number of breaks for the control group is by definition zero. Without a damaging agent control mtDNA would have no breaks and this is the standard against which mtDNA which has been exposed to a damaging agent is compared. Break frequency was determined as $-\ln$ (band intensity after treatment with either TRO or ROSI/band intensity of control).

Cell viability

The CellTiter 96 assay (Promega), a colorimetric method for determining the number of viable cells by assessing mitochondrial function, was performed 24 h after exposure to different concentrations of TRO or ROSI (18). The reagent contains a tetrazolium compound [3-(4,5-dimethylthiazol-2-yl)-5-(3-carboxymethoxyphenyl)-2-(4-sulphophenyl)-2H-tetrazolium, inner salt; MTS] and an electron-coupling reagent (phenazine methosulfate). MTS is bioreduced by the dehydrogenase enzymes found in metabolically-active cells into a formazan product soluble in tissue culture medium. The quantity of formazan product measured by the amount of 490 nm absorbance is directly proportional to the number of living cells in culture. The reagent is added to culture wells and the cells are incubated for 2 h. Optical density (OD) was read at 490 nm in a microplate reader. Data are indicated as percentage of untreated controls.

Protein transduction

MTS-EndoIII-TAT protein expression and purification was performed as described previously (19). For expression analysis, human hepatocytes were grown in 60 mm dishes. Different concentrations (10, 25 and 50 μg) of MTS-EndoIII-TAT in the elution buffer were added directly to the HHCM and incubated either for 3 or 24 h. Control cells were incubated for 24 h in media containing elution buffer (EB) only. After the indicated time, mitochondrial

fractions were isolated. For the viability study, cells were grown in 24 well plates and, prior to addition of TRO, were preincubated with 25 µg/ml of MTS-EndoIII-TAT for 3 h. Control cultures were preincubated with the same amount of EB for the same time.

Measurement of ATP levels

Cells were grown in 24-well culture plates and treated with TRO. To determine the total cellular ATP concentration, an ATP bioluminescence assay kit (Roche Molecular Biochemicals, Mannheim, Germany) was used. This kit employs a well-established technique which uses the ATP dependency of the light emitting luciferase catalyzed oxidation of luciferin for the measurement of extremely low concentrations of ATP (20). The emitted light is linearly related to the ATP concentration and is measured using a luminometer. Values are shown as a percentage of untreated control.

DNA Fragmentation Assay

The presence of fragmented nuclear DNA in the cytoplasmic fraction of cell lysates was assessed by measuring DNA associated with nucleosomal histones using a specific two-site ELISA with an antihistone primary antibody and a secondary anti-DNA antibody according to the manufacturer's instructions. Briefly, the cells were grown in 24-well culture plates, treated with TRO, washed twice with PBS, and incubated with 0.5 ml of lysis buffer for 20 min at room temperature. After centrifugation to remove nuclei and cellular debris, the supernatants were diluted 1:4 with lysis buffer and 20 µl from each sample were analyzed by ELISA. The intensity of the color that developed was determined by measuring the absorbance at 405 nm, while that at 490 nm was used as a blank (reference wavelength). Each condition was assessed at least in duplicate, and experiments were repeated three times independently.

Preparation of cellular fractions and Western blot analysis

Mitochondrial and cytosolic protein fractions were isolated from one 60 mm or 100 mm dish, respectively, as described previously (16,17). The protein concentration was determined using the Bio-Rad protein dye micro-assay according to the manufacturer's recommendations (Bio-Rad, Hercules, CA). SDS-polyacrylamide gel electrophoresis and transfer of separated proteins to PVDF-membranes were performed as previously described (16,17) with some minor modifications. Blocking and antibody immunoblotting were performed in 5% nonfat dry milk and Tris-buffered saline with 0.1% Tween 20 (TBS-T). TBS-T and TBS were used for washing. Anti-cytochrome *c* monoclonal antibody was purchased from PharMingen (San Diego, CA); caspase 3 (Cell Signaling; Beverly, MA); anti-actin and anti hemagglutinin (HA) antibodies were obtained from Sigma (Sigma, St. Louis, MO). Complexes formed by these antibodies were detected with horseradish peroxidase conjugated anti-mouse IgG or anti-rabbit IgG antibodies (Promega, Madison, WI) using chemiluminescent reagents (SuperSignal, Pierce, Rockford, IL).

Statistical analysis

Data are expressed as means \pm SE. Statistical significance was determined using one way ANOVA followed by Bonferroni analysis. Viability data for the PPAR γ antagonist, NAC and MTS-EndoIII-TAT were compared to TRO-only data using unpaired Student's t-test to determine statistical significance. The results were considered to be statistically significant if $P < 0.05$ was achieved.

Results

TRO, but not ROSI, induced mtDNA damage in human hepatocytes

To determine whether TRO or ROSI caused damage to mtDNA, a quantitative Southern blot technique was employed. The two groups were treated as described in the methods, and mtDNA integrity assessed at 24 h (Fig. 1, panels A-D). We found that TRO caused significant damage to mtDNA in human hepatocytes after 24 h of exposure, ranging from a low of approximately 2 breaks per 10^5 normal nucleotides to 1 break per 10^4 nucleotides (Fig. 1, panels A and C). The same concentrations of ROSI damaged mtDNA to a much lesser extent (Fig. 1, panels B and D). The results (Fig. 1, panels B and D) obtained from these studies revealed that the number of mtDNA breaks in ROSI-treated cultures was approximately 3-5 fold less than in TRO treated cells.

TRO, but not ROSI, decreased cell viability

To evaluate whether the observed increase in mtDNA damage affected viability following exposure to TRO, cell viability was assessed 24 h after exposure to 5-50 μ M TRO (Fig. 2A). For comparison, human hepatocytes were treated with the same concentrations of ROSI (Fig. 2B). Cell viability progressively decreased as the concentration of TRO was increased (Fig. 2A), whereas the ROSI treatment had no effect on cellular viability, even at the highest concentration used (Fig. 2B).

Effect of an antioxidant and a PPAR γ antagonist on cell viability

To determine whether ROS generation is involved in TRO-induced cytotoxicity, the effect of an antioxidant, NAC (a precursor compound for glutathione formation) on cell viability was evaluated. As shown in Fig. 3A, 10 mM NAC significantly diminished TRO-induced cytotoxicity, suggesting that ROS generation is responsible for cell death. To evaluate whether the PPAR γ activation is responsible for the TRO-induced decrease in hepatocyte viability, cells were treated with TRO in the presence of 10 μ M of the PPAR γ antagonist GW9662. The results, shown in Fig. 3B, indicate that GW9662 did not protect hepatocytes from TRO-induced toxicity, demonstrating that TRO-induced cell toxicity is PPAR γ -independent.

Enhancing mtDNA repair reduced TRO-induced cell death

Previously, we have reported conditional expression of the *Escherichia coli* Endo III gene in HeLa cells and targeting of this DNA repair protein to mitochondria (21). Because stable transfection with a plasmid is difficult in primary culture, we used a protein transduction strategy to deliver the repair protein to hepatocytes. To accomplish this we used the 11 amino acid Protein Transduction Domain (PTD) from the HIV-1 TAT protein (TAT-PTD). When the TAT-PTD is fused to other proteins, it confers to them the ability to be taken up into cells (22). To send the transduced proteins to mitochondria we used the same MTS (from human MnSOD) as has been used in the previous studies (21). The construct used for expressing and purifying recombinant EndoIII is outlined in Fig. 4A. We used oligonucleotides to assemble the synthetic MTS positioned on the N-terminus of the protein followed by the EndoIII sequence. For the C-terminus of the protein, we used another synthetic construct containing the TAT-PTD and ten consecutive histidine residues for purification by immobilized metal affinity chromatography. Also, to facilitate the detection of recombinant EndoIII, a hemagglutinin tag (HA) was included. The complete fusion construct was made with several rounds of PCR amplification. The PCR products were cloned and their sequence verified to exclude errors introduced by PCR. The fusion constructs were placed under the control of the inducible T7 lac promoter in pET series vectors (Novagen) and introduced into *E. coli* BL21 cells for expression. The bacteria were grown in liquid cultures, collected by centrifugation, and used for subsequent purification of the recombinant protein as previously described (19).

Because fusion constructs contained a stretch of ten histidines, we were able to purify these proteins from the *E. coli* lysates by employing a nickel-NTA column (Qiagen) with buffer containing imidazole. The purity of the eluted protein was assessed by SDS-PAGE and Western blot (data not shown). N-terminal sequencing verified that the purified protein had intact MTS. The activity of the fusion protein was assessed using an enzyme activity assay (data not shown) prior to adding to the cells as described in (21) except that radiolabelled apurinic site-containing oligonucleotide was used instead of radiolabelled thymine glycol containing oligonucleotide. Prior to the viability study, we evaluated whether MTS-EndoIII-TAT protein could be transduced into hepatocytes and targeted to mitochondria. Hence, hepatocytes were incubated with MTS-EndoIII-TAT (10, 25 and 50 μg) at two time points (3 and 24 h) and mitochondrial fractions were isolated by differential centrifugation as described in the experimental procedures section. Fig. 4B shows the results of Western blot analysis which was performed using anti-HA antibody. The presence of distinct bands (about 30 kD) in mitochondrial extracts isolated from cells transduced with EndoIII confirms that the transduced protein is localized in mitochondria (Fig.4B, top panel). Mitochondrial localization was verified by immunodetection of the mitochondrial protein cytochrome c (Fig.4B, bottom panel). The effect of MTS-EndoIII-TAT protein transduction on TRO-induced cell toxicity is shown in Fig. 4C. There is an increase in cell viability in the MTS-EndoIII-TAT pretreated cells.

TRO decreased cellular ATP concentrations

ATP concentrations were assessed in either TRO- or ROSI-treated groups at 24 h. A progressive decrease was seen at concentrations between 5 and 50 μM for TRO-treated hepatocytes after 24 h (Fig. 5A). ROSI treatment did not decrease cellular ATP levels (Fig. 5B).

TRO induced apoptosis in human hepatocytes

To determine whether exposure to TRO induced normal human hepatocytes to undergo apoptosis, a DNA fragmentation assay was performed (Fig. 6A). Beginning with the lowest concentration, an increase in DNA fragmentation was seen in cultures treated with 5-20 μM . We were unable to measure the DNA fragmentation at 35 and 50 μM because of the high percentage of cells that detached and floated off of the culture vessel at those concentrations. Additionally, apoptosis was confirmed by assessing caspase 3 activation (Fig. 6B). There is a significant decrease in the total caspase 3 level in the fractions isolated from hepatocytes treated with 35 or 50 μM TRO (Fig. 6B). To determine whether the induction of apoptosis was via a mitochondrial-induced mechanism, the release of cytochrome c into the cytosol was evaluated using Western blot analysis (Fig. 6C). Beginning at 20 μM , an increasing amount of cytochrome c was found in the cytosol of hepatocytes exposed to TRO for 24 h.

Discussion

In this study we investigated the effect of TRO and ROSI, which are PPAR γ agonists, on mtDNA damage, mitochondrial dysfunction and cellular viability in primary human hepatocytes. We found that only TRO caused a significant increase in mtDNA damage and decrease in ATP concentrations, which was associated with a significant decline in cellular viability. ROSI, which is another PPAR γ agonist and is still on the market, caused much less damage to mtDNA and had no effect on both ATP levels and cellular viability. It is worth noting that since our discovery, almost twenty years ago, that mitochondria can repair some types of damage to its DNA (23), we have actively studied damage and repair in mtDNA resulting from exposure to a variety of toxins. TRO is the most potent mtDNA toxin, on a molar basis, of any of the toxins we have studied. Maximal plasma concentrations in humans after treatment with therapeutic doses of TRO have been reported to be 0.4-2.4 mg/l (0.9-6.4 μM) (24). The concentrations of TRO used in our study were higher than plasma concentrations

under therapeutic conditions in humans. However, it has been reported that TRO is concentrated in the liver of animals after oral administration (25). Also, clinically, TRO was administered for a long term, thus likely increasing its accumulation in the human liver. If TRO accumulated in human liver during treatment, as appears likely, the hepatocytes would be exposed to higher concentrations of the drug than those measured in plasma. For comparison, we chose to use equimolar doses of ROSI to those used for TRO. ROSI is a much more potent PPAR γ agonist and, therefore, the doses we used are well above the therapeutic doses used. This makes the lack of toxicity even more striking.

The reason that TRO is more toxic than other TZDs is likely due to its difference in chemical structure. In addition to having a TZD ring, which is essential for enhancing PPAR γ function, it also has the chroman ring of vitamin E. This chroman ring can be metabolized to a quinone, which can undergo redox cycling to generate ROS. It has been shown that one of the metabolites of TRO is a TZD-quinone. It is possible that this TZDquinone can be further metabolized to undergo ring opening and thus form a bifunctional reactive intermediate which could covalently bind to DNA and proteins and continue to redox cycle via its quinone moiety to produce localized ROS. While these structural issues relating to TRO have yet to be fully resolved, the present work with NAC clearly supports the concept that TRO elicits its unique toxic properties through the generation of ROS (26). Our data is in good agreement with previous studies which provided evidence that TRO induced ROS production in human hepatocytes (10,12).

To confirm that the effect of TRO treatment on cell viability was PPAR γ -independent, we utilized the potent and selective PPAR γ antagonist GW9662 (15). In our experiments, GW9662 did not decrease TRO-induced cytotoxicity, indicating that this drug cytotoxicity is PPAR γ -independent in human hepatocytes.

The involvement of mitochondria in apoptosis was established by the finding that cytochrome c was translocated to the cytosol following exposure to TRO. Previous studies by our research group, as well as those of others, have established that damage to mtDNA following oxidative stress is an initiator of cell death (21,27-31). These studies have shown that when mtDNA repair is enhanced by targeting a recombinant DNA repair enzyme to mitochondria, there is a decrease in oxidative stress-induced cell death. Previously we have shown that conditional targeting of EndoIII to mitochondria enhanced repair of oxidative damage to mtDNA and increased cellular resistance to ROS (21). In the present study we have used the same DNA repair protein, EndoIII from *E.coli*, but utilized a protein transduction technique, due to the difficulty in obtaining stably-transfected clones in cells in primary culture. We have utilized this approach previously for a different bacterial DNA repair enzyme, Exonuclease III (19). In the present study we show that the recombinant protein MTS-EndoIII-TAT can be transduced into human hepatocytes and targeted into mitochondria. Also, targeting MTS-EndoIII-TAT into mitochondria of human hepatocytes increases cell viability after TRO treatment, establishing that mtDNA damage is involved in the initiation of TRO-induced toxicity.

The work reported here adds to the growing body of evidence which indicates that the non-receptor mediated effects of TRO act through interactions with mitochondria (32). Initially, it was found that there was a rapid depolarization of the mitochondrial membrane ($\Delta\Psi$) when a variety of cells, including hepatocytes, were exposed to TRO, which was associated with an increase in cytosolic calcium (11) and swelling of mitochondria (33). Additionally, it was observed that the loss of membrane potential correlated with a drop in ATP (11). As a result of this mitochondrial dysfunction, it has been reported that the production of ROS is increased and there is a concomitant rise in the initiation of apoptosis. By integrating the previous work by others with that reported here, we believe it is possible to develop a mechanistic explanation for the extra receptor properties of TRO (Fig. 7). The TRO-induced production of ROS (initial

ROS, Fig. 7) leads to the oxidation of key components within mitochondria, including mtDNA. This DNA is more vulnerable to damage caused by ROS than its nuclear counterpart because of its lack of protective histones and close location to the source of ROS generation. The exact origin of initial TRO-induced oxidative stress still needs to be elucidated (question mark in the Fig.7). We can speculate that candidate sites of ROS production are mitochondria or membrane-bound enzymes such as NADPH oxidases, or redox of TRO itself. The oxidative damage to mtDNA causes an increase in the production of ROS (secondary ROS, Fig. 7) by causing aberrant respiratory complex formation through the lack of coordination between components of the electron transport chains coded by mtDNA and those coded by nuclear DNA. The resultant production of ROS is able to initiate the formation of a vicious cycle in which ROS cause damage to mtDNA which causes further impairment in the formation of respiratory complexes and a concomitant increase in ROS production which leads to even more damage to mtDNA. As the damage to mtDNA rises, there is a concomitant drop in ATP production resulting from the impairment of the two electron reduction. This reduction in electron transport causes a decrease in mitochondrial depolarization. This link between mtDNA damage and $\Delta\Psi$ has been established by Santos and colleagues (34). As this process continues, there will be a diminution in cellular functions caused by the drop in ATP production. Depletion of mtDNA is known to suppress ATP synthesis and leads to defects in cellular function (35). Moreover, dysfunction of electron transport chains could cause additional production of ROS (secondary ROS, Fig. 7) and, in this way, enhance the cellular signals to initiate cell death. One of the manifestations of this decreased cellular function in hepatocytes is the inhibition of the bile salt export pump that has been observed following treatment with TRO (26). As this deleterious process continues, the mitochondrial permeability transition pore will open and the cell will die either by apoptotic mechanisms if ATP is still present in sufficient quantities, or necrotic mechanisms, if ATP has been depleted.

What is novel about our work is that we are reporting a potential mechanism implicating TRO-induced mtDNA damage as an initiator of a vicious cycle of events which leads to a decline in cellular function and ultimately to cell death. Furthermore, we demonstrate that by enhancing mtDNA repair we can block this mechanism of toxicity. This work suggests a new method for blocking the toxicity of this and other drugs and toxins that work through similar mechanisms.

ACKNOWLEDGEMENTS

We are grateful to Dr. Inna Shokolenko and Sergei Musiyenko for providing MTS-EndoIII-TAT protein. This research was supported by National Institutes of Health Grants ES03456 (G.L.W.), ES05865 (S.P.L), and DK073808 (L.I.R.).

ABBREVIATIONS

DMSO, dimethylsulfoxide
EB, elution buffer
EndoIII, Endonuclease III
HA, hemagglutinin
HHCM, human hepatocyte complete media
mtDNA, mitochondrial DNA
MTS, mitochondrial translocation sequence
NAC, N-acetyl cysteine
PPAR γ , peroxisome proliferator-activated receptor γ
PTD, protein transduction domain
ROS, reactive oxygen species
ROSI, rosiglitazone
TZDs, thiazolidinediones
TRO, troglitazone

References

1. Saltiel AR, Olefsky JM. Thiazolidinediones in the treatment of insulin resistance and type II diabetes. *Diabetes* 1996;45:1661–1669. [PubMed: 8922349]
2. Fujiwara T, Yoshioka S, Yoshioka T, Ushiyama I, Horikoshi H. Characterization of new oral antidiabetic agent CS-045. Studies in KK and ob/ob mice and Zucker fatty rats. *Diabetes* 1988;37:1549–1558. [PubMed: 3053303]
3. Nolan JJ, Ludvik B, Beerdsen P, Joyce M, Olefsky J. Improvement in glucose tolerance and insulin resistance in obese subjects treated with troglitazone. *N. Engl. J. Med* 1994;331:1188–1193. [PubMed: 7935656]
4. Lehmann JM, Moore LB, Smith-Oliver TA, Wilkison WO, Willson TM, Kliewer SA. An antidiabetic thiazolidinedione is a high affinity ligand for peroxisome proliferator-activated receptor gamma (PPAR gamma). *J. Biol. Chem* 1995;270:12953–12956. [PubMed: 7768881]
5. Schoonjans K, Staels B, Auwerx J. The peroxisome proliferator activated receptors (PPARS) and their effects on lipid metabolism and adipocyte differentiation. *Biochim. Biophys. Acta* 1996;1302:93–109. [PubMed: 8695669]
6. Chojkier M. Troglitazone and liver injury: in search of answers. *Hepatology* 2005;41:237–246. [PubMed: 15657914]
7. Haskins JR, Rowse P, Rahbari R, de la Iglesia FA. Thiazolidinedione toxicity to isolated hepatocytes revealed by coherent multiprobe fluorescence microscopy and correlated with multiparameter flow cytometry of peripheral leukocytes. *Arch. Toxicol* 2001;75:425–438. [PubMed: 11693184]
8. Tirmenstein MA, Hu CX, Gales TL, Maleeff BE, Narayanan PK, Kurali E, Hart TK, Thomas HC, Schwartz LW. Effects of troglitazone on HepG2 viability and mitochondrial function. *Toxicol. Sci* 2002;69:131–138. [PubMed: 12215667]
9. Narayanan PK, Hart T, Elcock F, Zhang C, Hahn L, McFarland D, Schwartz L, Morgan DG, Bugelski P. Troglitazone-induced intracellular oxidative stress in rat hepatoma cells: a flow cytometric assessment. *Cytometry A* 2003;52:28–35. [PubMed: 12596249]
10. Shishido S, Koga H, Harada M, Kumemura H, Hanada S, Taniguchi E, Kumashiro R, Ohira H, Sato Y, Namba M, Ueno T, Sata M. Hydrogen peroxide overproduction in megamitochondria of troglitazone-treated human hepatocytes. *Hepatology* 2003;37:136–147. [PubMed: 12500198]
11. Bova MP, Tam D, McMahon G, Mattson MN. Troglitazone induces a rapid drop of mitochondrial membrane potential in liver HepG2 cells. *Toxicol. Lett* 2005;155:41–50. [PubMed: 15585358]
12. Lim LM, Liu J, Go ML, Boelsterli UA. The mitochondrial superoxide/thioredoxin-2/Ask1 signaling pathway is critically involved in troglitazone-induced cell injury to human hepatocytes. *Toxicol. Sci* 2008;101:341–349. [PubMed: 17975114]
13. Okura T, Nakamura M, Takata Y, Watanabe S, Kitami Y, Hiwada K. Troglitazone induces apoptosis via the p53 and Gadd45 pathway in vascular smooth muscle cells. *Eur. J. Pharmacol* 2000;407:227–235. [PubMed: 11068018]
14. Jung JY, Yoo CI, Kim HT, Kwon CH, Park JY, Kim YK. Role of mitogen-activated protein kinase (MAPK) in troglitazone-induced osteoblastic cell death. *Toxicology* 2007;234:73–82. [PubMed: 17363128]
15. Leesnitzer LM, Parks DJ, Bledsoe RK, Cobb JE, Collins JL, Consler TG, Davis RG, Hull-Ryde EA, Lenhard JM, Patel L, Plunket KD, Shenk JL, Stimmel JB, Therapontos C, Willson TM, Blanchard SG. Functional consequences of cysteine modification in the ligand binding sites of peroxisome proliferator activated receptors by GW9662. *Biochemistry* 2002;41:6640–6650. [PubMed: 12022867]
16. Grishko V, Rachek L, Musiyenko S, LeDoux SP, Wilson GL. Involvement of mtDNA damage in free fatty acid-induced apoptosis. *Free Radic. Biol. Med* 2005;38:755–762. [PubMed: 15721986]
17. Rachek LI, Musiyenko SI, LeDoux SP, Wilson GL. Palmitate induced mtDNA damage and apoptosis in L6 rat skeletal muscle cells. *Endocrinology* 2007;148:293–299. [PubMed: 17023529]
18. Cory AH, Owen TC, Barltrop JA, Cory JG. Use of an aqueous soluble tetrazolium/formazan assay for cell growth assays in culture. *Cancer Commun* 1991;3:207–212. [PubMed: 1867954]

19. Shokolenko IN, Alexeyev MF, LeDoux SP, Wilson GL. TAT-mediated protein transduction and targeted delivery of fusion proteins into mitochondria of breast cancer cells. *DNA Repair* 2005;4:511–518. [PubMed: 15725631]
20. Crouch SP, Kozlowski R, Slater KJ, Fletcher J. The use of ATP bioluminescence as a measure of cell proliferation and cytotoxicity. *J. Immunol. Methods* 1993;160:81–88. [PubMed: 7680699]
21. Druzhyna NM, Hollensworth SB, Kelley MR, Wilson GL, Ledoux SP. Targeting human 8-oxoguanine glycosylase to mitochondria of oligodendrocytes protects against menadione-induced oxidative stress. *Glia* 2003;42:370–378. [PubMed: 12730957]
22. Rachek LI, Grishko VI, Alexeyev MF, Pastukh VV, LeDoux SP, Wilson GL. Endonuclease III and endonuclease VIII conditionally targeted into mitochondria enhance mitochondrial DNA repair and cell survival following oxidative stress 2004;32(10):3240–3247.
23. Schwarze S, Ho A, Vocero-Akbani A, Dowdy S. In vivo protein transduction: delivery of a biologically active protein into the mouse. *Science* 1999;285:1569–1572. [PubMed: 10477521]
24. Pettepher CC, LeDoux SP, Bohr VA, Wilson GL. Repair of alkali-labile sites within the mitochondrial DNA of RINr 38 cells after exposure to the nitrosourea streptozotocin. *J. Biol. Chem* 1991;266:3113–3117. [PubMed: 1825207]
25. Spencer CM, Markham A. Troglitazone. *Drugs* 1997;54:89–101. [PubMed: 9211083]discussion 102
26. Kawai K, Kawasaki-Tokui Y, Odaka T, Tsuruta F, Kazui M, Iwabuchi H, Nakamura T, Kinoshita T, Ikeda T, Yoshioka T, Komai T, Nakamura K. Disposition and metabolism of the new oral antidiabetic drug troglitazone in rats, mice and dogs. *Arzneimittelforschung* 1997;47:356–368. [PubMed: 9150855]
27. Smith MT. Mechanisms of troglitazone hepatotoxicity. *Chem. Res. Toxicol* 2003;16:679–687. [PubMed: 12807350]
28. Rachek LI, Grishko VI, Musiyenko SI, Kelley MR, LeDoux SP, Wilson GL. Conditional targeting of the DNA repair enzyme hOGG1 into mitochondria. *J. Biol. Chem* 2002;277:44932–44937. [PubMed: 12244119]
29. Druzhyna NM, Musiyenko SI, Wilson GL, LeDoux SP. Cytokines induce nitric oxide-mediated mtDNA damage and apoptosis in oligodendrocytes. Protective role of targeting 8-oxoguanine glycosylase to mitochondria. *J. Biol. Chem* 2005;280:21673–21679. [PubMed: 15811855]
30. Ruchko M, Gorodnya O, LeDoux SP, Alexeyev MF, Al-Mehdi AB, Gillespie MN. Mitochondrial DNA damage triggers mitochondrial dysfunction and apoptosis in oxidant-challenged lung endothelial cells. *Am. J. Physiol. Lung. Cell. Mol. Physiol* 2005;288:L530–535. [PubMed: 15563690]
31. Rachek LI, Grishko VI, LeDoux SP, Wilson GL. Role of NO-induced mtDNA damage in mitochondrial dysfunction and apoptosis. *Free Radic. Biol. Med* 2006;5:754–762. [PubMed: 16520228]
32. Rachek LI, Thornley NP, Grishko VI, LeDoux SP, Wilson GL. Protection of INS-1 Cells From Free Fatty Acid-Induced Apoptosis by Targeting hOGG1 to Mitochondria. *Diabetes* 2006;55(4):1022–1028. [PubMed: 16567524]
33. Feinstein DL, Spagnolo A, Akar C, Weinberg G, Murphy P, Gavriluk V, DelloRusso C. Receptor independent actions of PPAR thiazolidinedione agonists: is mitochondrial function the key? *Biochem Pharmacol* 2005;70:177–188. [PubMed: 15925327]
34. Masubuchi Y, Kano S, Horie T. Mitochondrial permeability transition as a potential determinant of hepatotoxicity of antidiabetic thiazolidinediones. *Toxicology* 2006;222:233–239. [PubMed: 16621215]
35. Santos JH, Hunakova L, Chen Y, Bortner C, Van Houten B. Cell sorting experiments link persistent mitochondrial DNA damage with loss of mitochondrial membrane potential and apoptotic cell death. *J. Biol. Chem* 2003;278:1728–1734. [PubMed: 12424245]
36. Chandel NS, Schumacker PT. Cells depleted of mitochondrial DNA (rho0) yield insight into physiological mechanisms. *FEBS Lett* 1999;454:173–176. [PubMed: 10431801]

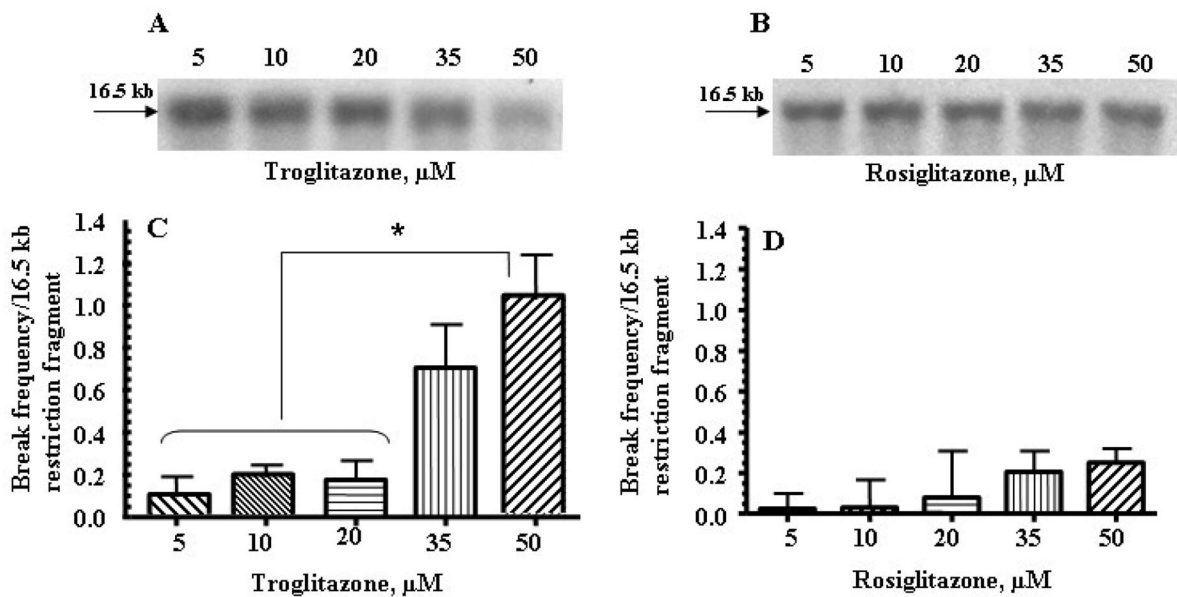


Fig. 1.

TRO damaged mtDNA to a greater extent than ROSI in primary human hepatocytes. (A and B) Representative autoradiograms from a Southern blot analysis of mtDNA from human hepatocytes after 24 h of treatment with the indicated concentrations of TRO (panel A) or ROSI (panel B). A decrease in band intensity represents an increase in mtDNA damage. (C and D) Break frequency per 16.5 kb fragment of mtDNA after 24 h of treatment with the indicated concentrations of TRO (panel C) or ROSI (panel D). Break frequency was determined as described in the "Materials and Methods". Intensity of the band was determined by densitometry, and break frequency was determined as $-\ln$ (band intensity after treatment with either TRO or ROSI/band intensity of control). The mean results \pm SE are shown. ($n > 3$). *, $P < 0.05$.

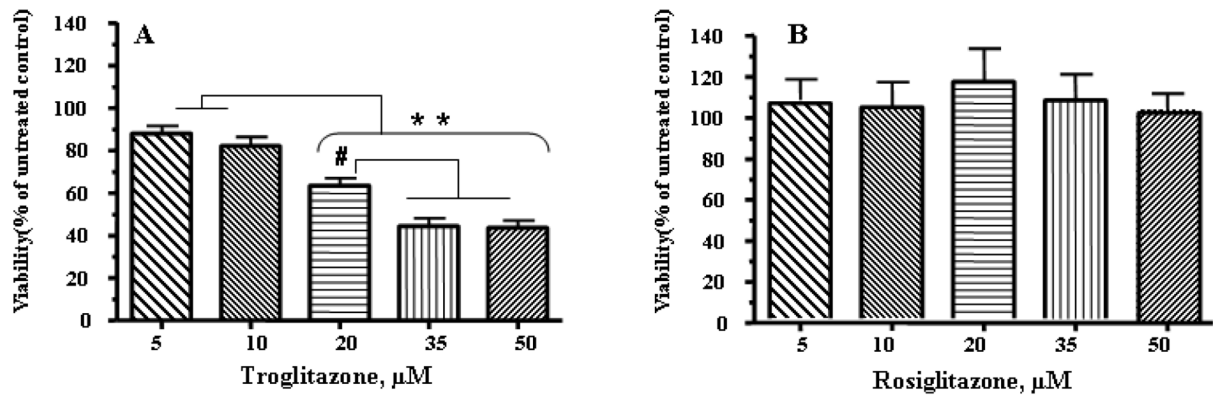


Fig. 2. TRO, but not ROSI, significantly diminished viability in primary cultures of human hepatocytes. (A) TRO significantly decreased viability in primary cultures of human hepatocytes after 24 h of treatment. (B) The same concentration of ROSI had no effect on hepatocyte viability. The mean results \pm SE are shown. ($n \geq 3$). #, $P < 0.01$, **, $P < 0.001$.

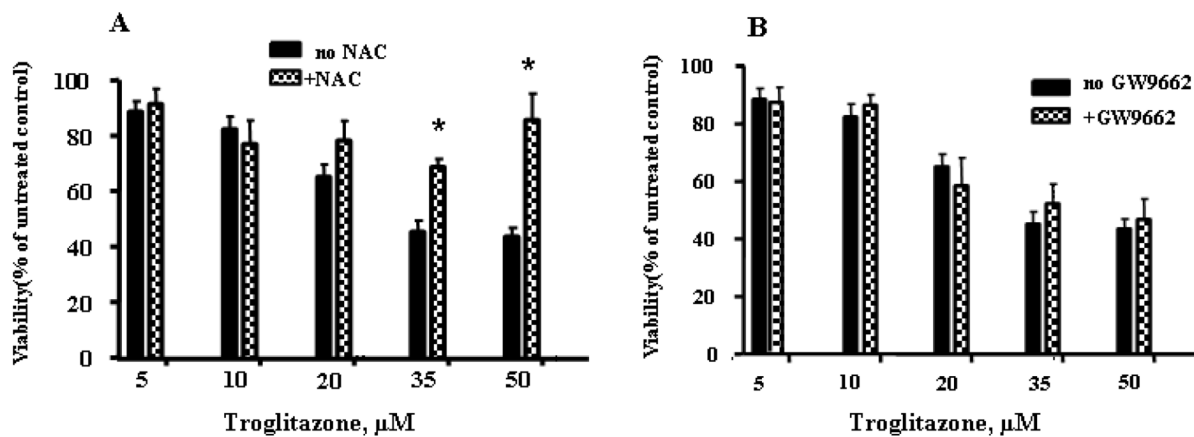


Fig. 3.

The effects of NAC and GW9662 on cell viability following treatment with TRO. Cells cultures were pretreated with either 10 μM GW9662 or 10 mM NAC for 15 min prior to addition of TRO. (A) 10 mM NAC significantly reversed the TRO-induced decline in cell viability. (B) 10 μM GW9662 did not block TRO-induced toxicity in human hepatocytes. The mean results \pm SE are shown. ($n \geq 3$). *, $P < 0.05$.

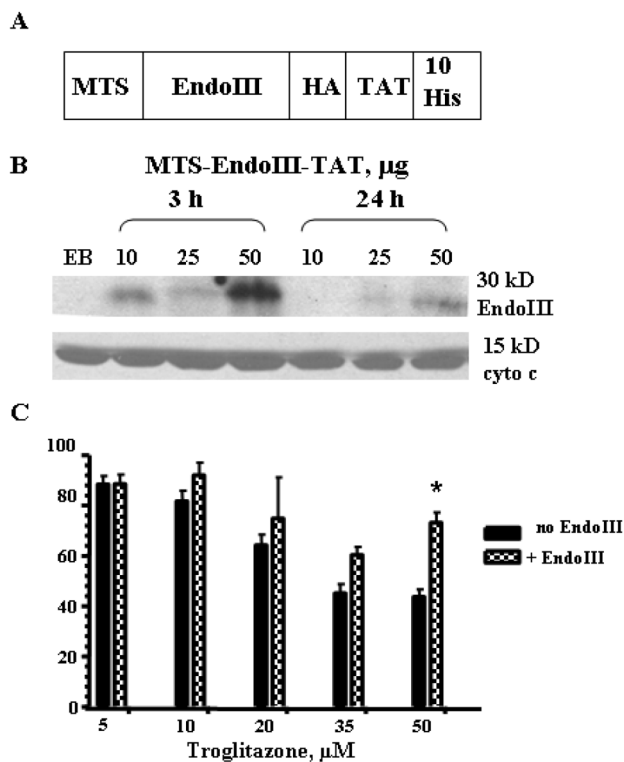


Fig. 4. Enhancing mtDNA repair by using MTS-EndoIII-TAT protein transduction reduced cell death after TRO treatment. (A) Schematic representation of the construct used for the expression of the fusion MTS-EndoIII-TAT protein. (B) Analysis of mitochondrial fractions after transduction of MTS-EndoIII-TAT. Western blots containing 40 μg of mitochondrial fractions after transduction of MTS-EndoIII-TAT protein for the indicated time points. Top panel shows the results of Western blot analysis using anti-HA antibodies. Immunodetection of cytochrome c was performed to show that recombinant proteins are in mitochondria (bottom panel). (C) MTS-EndoIII-TAT protein transduction enhanced cell viability after TRO treatment. The mean results \pm SE are shown. ($n \geq 3$). *, $P < 0.05$.

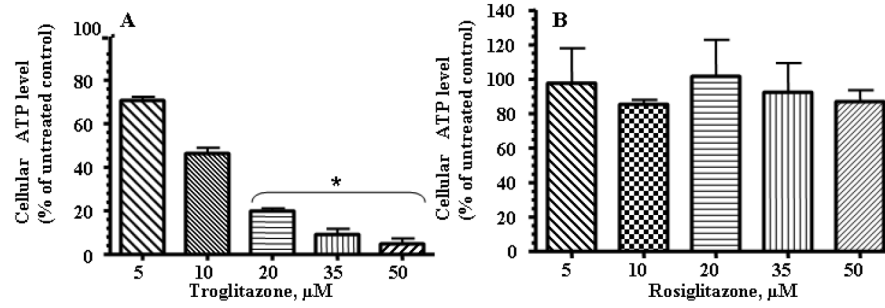


Fig. 5. TRO significantly decreased ATP levels in human hepatocytes. Cells were treated with the indicated concentration of TRO (panel A) or ROSI (panel B) for 24 h and ATP production was measured. The mean results \pm SE are shown. ($n \geq 3$). *, $P < 0.05$.

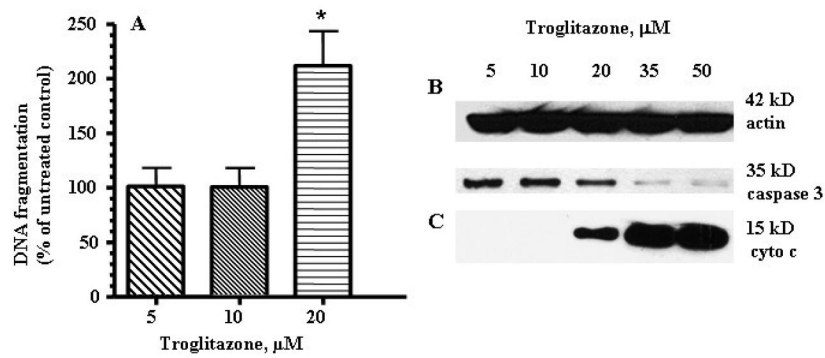


Fig. 6. TRO induced apoptosis, caspase 3 activation and cytochrome c release from mitochondria in human hepatocytes. (A) DNA fragmentation was measured by an ELISA assay using absorbance (OD 405-490 values). Culture of human hepatocytes for 24 h in the presence of TRO caused fragmentation of DNA. The mean \pm SE are shown (n=3). *, $P < 0.05$. (B) Caspase 3 antibodies were used to recognize the full length (35-kD) fragment. (C) Western blots for cytochrome c were performed on the cytosolic protein fraction from human hepatocytes exposed to different concentrations of TRO for 24 h. Equal loading was confirmed using anti actin antibody.

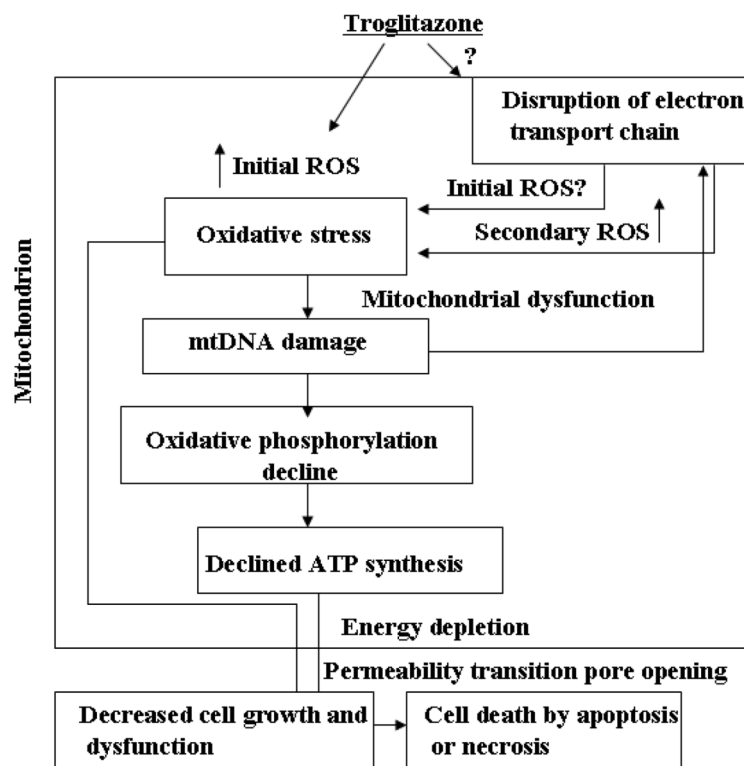


Fig. 7. Schematic model of the proposed effects of TRO-induced mitochondrial dysfunction in the development of hepatotoxicity. This schematic describes the model discussed in detail in the text. TRO-induced production of ROS (initial ROS) causes damage to all components within the mitochondria, including mtDNA. MtDNA damage results in alterations in mtDNA transcription and reduction in the number of mitochondrially-encoded proteins, leading to decline in ATP production and impaired electron transport. The impaired electron transport causes additional ROS production (secondary ROS), thus establishing a vicious cycle since any damage to the respiratory chain may enhance ROS production. This increased oxidative stress and decreased ATP generation exacerbates the mitochondrial dysfunction, heightens the oxidative stress to all mitochondrial components, and further intensifies the TRO-induced oxidative stress in human hepatocytes until apoptosis or necrosis results.